Comparison of Brushless DC Motor Drive Performance fed by Two Different Front End DC – DC Power Converters

Santhosh P[1,2] and Vijayakumar P[3]

[1]Ph.D Scholar, Anna University, Chennai, [2]*Assistant Professor, SVS College of Engineering, Coimbatore.*
[3]*Professor, Karpagam College of Engineering, Coimbatore.*

a) santhosivam@gmail.com, b) vijay.pvk72@gmail.com

Abstract— The importance of Brushless DC motors has been increasing across domestic and industrial applications for a multitude of advantages. This paper concerns the implementation of the brushless DC motor with two different front end DC–DC converter topologies, canonical switching cell (CSC) converter and Landsman converter. The performance of the motor in these topologies are compared. MATLAB/Simulink is used to design and simulate the converter circuits. The motor parameters under discussion are stator back emf, rotor speed and its ripple factor. A conscious effort has been made to present the parameter values in an easily comparable and a conclusion has been drawn on the best possible topology among these two to enable the motor to function efficiently and help us get desirable results when the motor is deployed in operation.

Key Terms: BLDC motor, DC–DC converters, CSC converter, Landsman converter.

I. Introduction

The exceptional performance, high reliability, ruggedness and wide range of speed control has made the BLDC motor gain its importance over the last decade [1-3]. Its application area is also wider, as it is well suited for all power ranges. Medical analysers, electric automotive and military applications are some of the key application areas of brushless dc motor in addition to house hold applications, motion control, industrial automation, ventilation and air conditioning applications [4,5]. The BLDC motors eliminates the sparking, noise, electro-magnetic interference (EMI) and maintenance problems associated with conventional DC motors, as these are synchronous motors with stator having three phase windings and a permanent magnets rotor with hall effect for position sensing. These enable easier commutation of the electronic commutator (VSI) feeding the motor. The drive is made simple, whereas supplying the VSI with appropriate DC link voltage is vital to achieve desired control over the drive. A dc link capacitor preceded by a diode bridge rectifier would serve the purpose. But, the problem is the high total harmonic distortion and injection of harmonics in the supply [10]. According to standard IEC 61000-3-2, these power quality indices are not acceptable. Literature reports many isolated and non-isolated power converters (single stage), which have minimal losses as the components are less in number[11,12]. Ozturk [13] and Wu [14] proposed a constant dc link fed VSI (using a boost topology) to feed the BLDC drive, whose speed is controlled by varying the VSI switching frequency. This results high switching loss due to the higher switching frequency of the PWM pulses. By having a variable DC link voltage the speed of the BLDC motor can be varied and at the mean time the switching losses can be reduced [19] as the VSI requires comparatively low switching frequency and need not change. A proposal of such concept with two current sensors in a SEPIC converter for feeding a BLDC motor is given in [18]. But the cost of the current sensors would increase the drive cost. Whereas, a single voltage sensor is required for operating the converter in voltage follower approach. Elimination of diode bridge rectifier (partial/complete) resulted in low conduction losses which made the bridgeless converters gain importance over the last decade [20]. Literature reveals many bridgeless converter configurations [20-30], starting from buck, boost and buck-boost converter (bridgeless configuration) each have their own limitations and losses. Hence, these are not preferable for wide range of voltage control (variable dc link voltage). The higher order converter configurations such as cuk [25-27], SEPIC[28,29] and Zeta[30] are widely used, still these have more number of switching components which leads to losses and emi. However less attention has been paid to canonical switching cell converter (CSC) and Landsman converter [17] even though they have good load regulation and lesser component count compared to non-isolated cuk converter [31-34]. Literature compares the conventional configurations with any of these converters to justify it is offering a better performance. It is essential to compare these trending converters to justify which offers an optimal performance among them. This paper presents performance comparison of these two converters (CSC and Landsman) driven BLDC drive.

II. BL-CSC converter fed BLDC motor drive

A bridgeless canonical switching cell converter based brushless dc motor drive is given in figure 1. The bridgeless configuration eliminates the diode bridge, resulting in reduction of conduction losses. The converter is designed such that the current through the input side inductors L_{i1} and L_{i2} are discontinuous and the intermittent capacitors (C_1 and C_2) voltage is continuous for a switching cycle. This enables the converter to operate in discontinuous conduction mode.

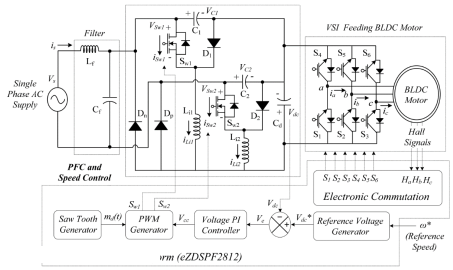

Figure 1 CSC converter with BLDC motor drive

Table 1 BLDC motor parameters

S. No.	Contents	Notation	Unit	Value
1	No. of poles	p		4
2	No. of phase	ph		3
3	Power	Prated	W	314
4	Voltage (DC link)	Vs	V	200
5	Speed	N	rpm	2000
6	Torque	T	N-m	1.5
7	Resistance (phase)	Rph	Ω	14.56
8	Inductance (phase)	Lph	mH	25.71
9	Torque Constant	Kt	Nm/A	0.74
10	Voltage Constant	Ke	V/krpm	78
11	Rotor Inertia	J	Nm/s2	1.8 x 10-4
12	Friction coefficient	B		7.5 x 10-4

III.Operation of the BL-CSC converter

The two cycle (+ve and -ve) operation of bridgeless canonical switching cell converter is shown in figure 2 to 7. The figures 2 to 4 depicts the operation of the converter in positive half cycle. As shown in figure, path of the current is through, S_{w1}, L_{i1} and D_p. Similarly, during the negative half cycle the current takes the path of switch S_{w2}, inductor L_{i2} and diode D_n as shown in figures 5 to 7.

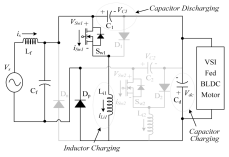

Figure 2 Mode P1

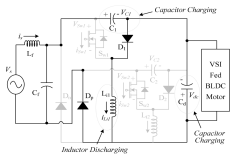

Figure 3 Mode P2

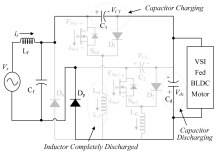

Figure 4 Mode P3

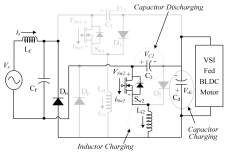

Figure 5 Mode N1

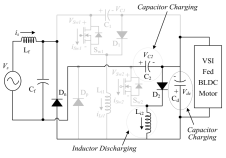

Figure 6 Mode N2

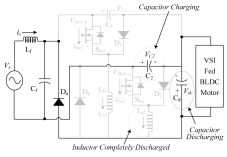

Figure 7 Mode N3

IV.CSC converter design

A 314W BLDC motor (Full specifications are given in Table 1) is preferred for the experimental studies. To feed the BLDC motor dive, a 500 W front end canonical switching cell converter is designed such that it provides a minimum dc link voltage of 70 V and a maximum of 200 V. This voltage variation facilitates spedd variation of the drive. The converter input voltage V_s is given by,

$$V_s(t) = V_m \sin(2\pi f_L t) = 220\sqrt{2}\sin(314t)V \quad (1)$$

V_m – peak input voltage (i.e. $\sqrt{2}V_S$),
f_L – line frequency (i.e. 50 Hz)

The equation (2) gives the instantaneous voltage acr oss any switch (S_{wn}) and inductor combination (L_{in}) an d the equation (3) gives the expression for output dc voltage of the converter [9].

$$V_{in}(t) = |V_m \sin(\omega t)| = |220\sqrt{2}\sin(314t)|V \quad (2)$$

$$V_{dc} = \frac{D}{(1-D)}V_{in} \quad (3)$$

D is the duty ratio, the instantaneous duty ratio D (t) depends on the instantaneous input voltage $V_{in}(t)$ and the dc output voltage, V_{dc} as given in (4)

$$D(t) = \frac{V_{dc}}{(V_{in}(t)-V_{dc})} = \frac{V_{dc}}{(|V_m \sin(\omega t)|-V_{dc})} \quad (4)$$

The instantaneous power (P_i) is taken as linear function of the dc output of the converter) as it varies with it and the speed of the drive also varies with the converter output voltage, therefore P_i is given as,

$$P_i = \left(\frac{P_{max}}{V_{dc\,max}}\right)V_{dc} \quad (5)$$

$V_{dc\ max}$ – maximum DC link voltage
P_{max} – rated power for the converter

Equation (5) is used to calculate the minimum output power (as 175 W) of the converter for a minimum dc link voltage of 70 V.

Input Inductor design (L_i)

The critical value of the input inductor L_{ic} is expressed as, [12]

$$L_{ic} = \frac{V_{in}(t)D(t)}{2I_{in}(t)f_s} = \frac{R_{in}D(t)}{2f_s} = \left(\frac{V_s^2}{P_i}\right)\frac{D(t)}{2f_s} \quad (6)$$

R_{in} represents the input resistance,
f_s is the switching frequency
P_i is the instantaneous power.

The inductor value and the switching frequency are inversely proportional, lower the inductor value higher is the switching frequency and the losses associated with the converter switches. Also, in DCIM operation the current stress on the converter switches will increase for low value of inductance. To have reduced stress on the switches and to achieve desired performance, the switching frequency of 20 kHz is selected. The $L_{ic\ min}$ is calculated at $V_{s\ min}$ (85 V) to

enable it to operate in universal voltage of 85 V to 270 V [17].

$$L_{ic\,min}=\left(\frac{V_{s\,min}^{2}}{P_{max}}\right)\frac{D(t)}{2f_s}=\left(\frac{85^2}{300}\right)\frac{0.7206}{2\times 20000}\approx 260\ \mu H \quad (7)$$

$L_{ic\ min}$ – minimum critical input inductor
$V_{s\ min}$ – minimum supply voltage

Duty ratio is determined at maximum converter output voltage (V_{dc} = 200 V) and at peak value of the minimum input voltage ($V_{s\ min\ (peak)} = 85\sqrt{2}$V). The value of $L_{ic\ min}$ the must be greater than L_{i1} and L_{i2}, therefore it is selected as $L_{i1} = L_{i2} = ¼ L_{ic\ min}$ =70µH (approx..) to enable discontinuous conduction mode.

Intermittent Capacitor design (C_i)

The value of C_i (intermittent capacitor) is calcul -ated at η_{max}, which occurs at $V_{dc\ max}$ and $V_{s\ max}$.

$$C_i=\frac{V_{dc}D(t)}{\Delta V_c(t)f_sR_L}=\frac{V_{dc}D(t)}{\eta\{V_{in}(t)+V_{dc}\}f_sR_L}$$

$$C_i=\frac{V_{dc\,max}D(t)}{\eta\{\sqrt{2}V_{s\,max}(t)+V_{dc}\}f_sR_L}$$

$$=\frac{200\ X\ 0.4481}{0.1\{(270\sqrt{2})+200\}\ 20000\ X\ 200}=0.385\ \mu F$$

V_C – voltage across the intermittent capacitor
η – ripple voltage C_i
R_L – load resistance, $R_L=V_{dc}^2/P_i$.
$C_i = C_1 = C_2$

The permitted η across the capacitor is 10 % of the capacitor voltage and hence the C_i is selected as 0.47 (nearest possible value).

DC Link Capacitor (C_d) design

The value of DC link capacitor is calculated as given in (10) [11], k is the permitted ripple in the dc link voltage.

$$C_d=\frac{I_{dc}}{2\omega\Delta V_{dc}}=\left(\frac{P_i}{V_{dc}}\right)\frac{1}{2\omega kV_{dc}} \quad (10)$$

$$C_d=\left(\frac{P_{min}}{V_{dc\,min}}\right)\frac{1}{2\omega\Delta V_{dc\,min}} \quad (11)$$

$$C_d=\left(\frac{175}{70}\right)\frac{1}{2x209x0.02x70}\approx 4272\mu F$$

The DC link capacitor with a nearest possible value of 4700µF is selected for this application.

Filter parameters (L_f and C_f) design

The higher order harmonics in the supply side is avoided by a low pass filter, the required capacitanc e and inductance values are calculated with (12) and (13) [36]. The Lf is designed consider the source impe dance.

$$C_{max}=\frac{I_m}{\omega_L V_m}\tan(\theta)=\frac{(P_o\sqrt{2}/V_s)}{\omega_L V_m}\tan(\theta)$$

$$C_{max}=\frac{(500\sqrt{2}/220)}{209\ X\ 220\sqrt{2}}\tan(1^0)=862.77\ nF \quad (12)$$

$$L_f=L_{req}+L_s=\frac{1}{4\pi^2 f_c^2 C_f}=L_{req}+0.05\left(\frac{1}{\omega_L}\right)\left(\frac{V_s^2}{P_o}\right)$$

$$L_{req}=\frac{1}{4\pi^2\ X\ (2000)^2 X\ 820X10^{-9}}\sim 0.05\left(\frac{1}{209}\right)\left(\frac{220^2}{500}\right)$$

$$L_{req}=15.435\ mH \quad (13)$$

f_c – cutoff frequency, $f_c=\frac{f_s}{10}$
f_s – switching frequency

the (possible) values of L_f and C_f are selected as 15 mH and 820 nF from the derived values.

Control of BL-CSC converter fed BLDC motor drive

The control of the drives is done in two stages, one at the front-end converter to control the dc link voltage (voltage follower approach) and the other for the electronic commutation (PWM control of VSI) for driving the motor.

Design of controller for Converter

The figure 8 shows the controller for the converter which has four major blocks, reference voltage generator, error voltage generator, PI controller and PWM generator.

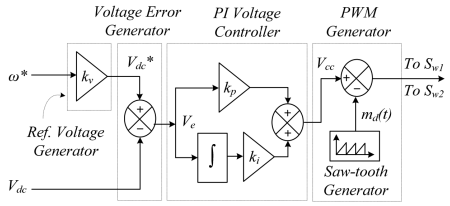

Figure 8 Control of BL-CSC converter.

The reference voltage generator give the reference voltage (V_{dc}^*) (14) which is the product of the motor constant (k_v) and speed of the motor (ω^*). The error voltage (V_e) (15) is the difference between the reference voltage (V_{dc}^*) and the converter output voltage (V_{dc}).

$$V_{dc}^{*}=k_v\omega^{*} \quad (14)$$

$$V_e(k)=V_{dc}(k)^{*}-V_{dc}(k) \quad (15)$$

The PI controller generates a controlled output voltage (V_{cc}) (16) from the error voltage as given in (16) and is fed to PWM generator, where it is compared with a high frequency carrier to generate PWM pulses to feed the converter switches as given in (17).

$$V_{cc}(k)=V_{cc}(k-1)+K_p\{V_e(k)-V_e(k-1)\}+K_iV_e(k) \quad (16)$$

$$for\ v_s>0;\ \begin{Bmatrix} if\ m_d<V_{cc}\ then\ S_{w1}='ON' \\ if\ m_d\geq V_{cc}\ then\ S_{w1}='OFF' \end{Bmatrix}$$

$$for\ v_s<0;\ \begin{Bmatrix} if\ m_d<V_{cc}\ then\ S_{w2}='ON' \\ if\ m_d\geq V_{cc}\ then\ S_{w2}='OFF' \end{Bmatrix} \quad (17)$$

S_{w1} and S_{w2} represent the gate signals to converter switches S_{w1} and S_{w2} respectively.

Controller for VSI to fed BLDC Motor

The electronic commutation of the BLDC motor is achieved by sensing the rotor position using the hall effect position sensor. Three hall effect sensors (H_a, H_b, H_c) are placed on the rotor in a span of 60^0. Based on the rotor position, the switching of the VSI is done as in table 2. The figure 9 shows conduction of two switched S_1 and S_4. The switching is done in such way, at point of time only switches are ON, energizing any two phases of the motor. This enables proper rotation and rotation in the correct direction.

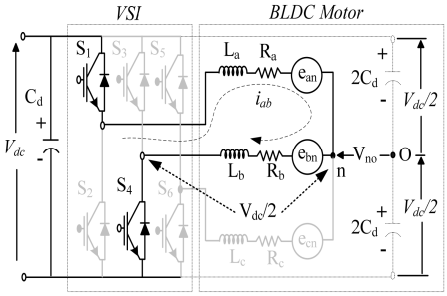

Figure 9 Conduction states of switches S1 and S4

Table 2 Switching states based on hall effect position signals.

θ(^{0})	Hall Signals			Switching States					
	H_a	H_b	H_c	S_1	S_2	S_3	S_4	S_5	S_6
NA	0	0	0	0	0	0	0	0	0
0 – 60	0	0	1	1	0	0	0	0	1
60 – 120	0	1	0	0	1	1	0	0	0
120 – 180	0	1	1	0	0	1	0	0	1
180 – 240	1	0	0	0	0	0	1	1	0
240 – 300	1	0	1	1	0	0	1	0	0
300 – 360	1	1	0	0	1	0	0	1	0
NA	1	1	1	0	0	0	0	0	0

V. Simulation of BL CSC fed BLDC drive

Simulink model

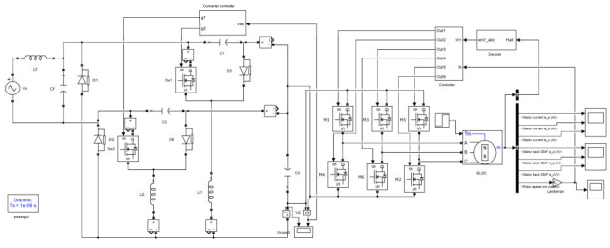

Figure 10 Simulink model of BL-CSC fed BLDC drive

The Simulink model of the CSC converter fed brushless DC motor drive is given in Figure 10. The functional parameters the back emf, stator current and speed of the of the motor along with the DC link voltage of the converter are observed and presented in the figures 11 to 14 respectively

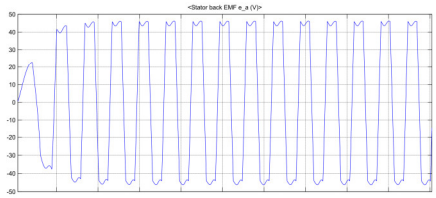

Figure 11 Stator back emf of CSC fed BLDC motor

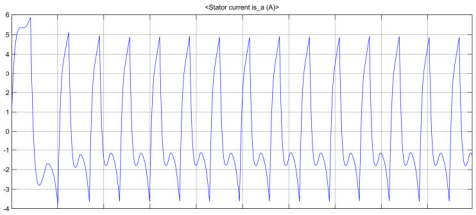

Figure 12 Stator current of CSC fed BLDC motor

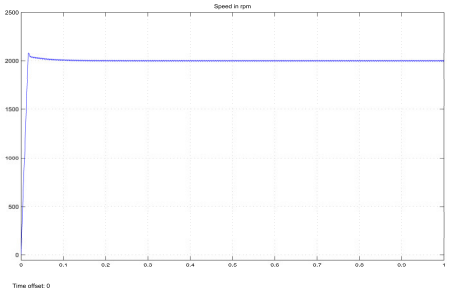

Figure 13 Speed Characteristics of CSC fed BLDC drive

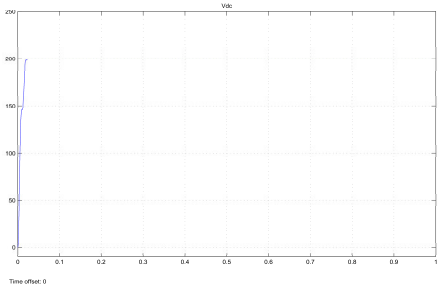

Figure 14 DC link voltage of CSC converter

Steady state response

The model is simulated with rated load torque with a dc link voltage of 200 V and 100 V, the corresponding speed and dc link voltage is given in Figure 15 and 16. Figure 17 gives speed characteristics of the model with 50 % of the rated load torque and a dc link voltage of 200 V. The time domain analysis in terms of integral square error, integral absolute error, integral time square error and integral time absolute error are obtained for the dc link

voltage of the converter and speed of the motor in addition to ripple factor and are tabulated in Table 3 and Table 4.

Table 3 Summary of errors and ripple factor of V_{dc} of CSC

S. No	DC link Voltage (V)	Load	IAE	ITAE	Ripple factor
1	200	Full load	1.75	0.141	0.0268
2	200	½ load	20.9	12.6	0.0817
3	100	Full load	0.60	0.680	0.0212

Table 4 Summary of errors and ripple factor of BLDC motor's speed

S. No	DC link Voltage (V)	Load	IAE	ITAE	Ripple factor
1	200	Full load	20.75	1.598	0.1853
2	200	½ load	10.75	0.923	0.1792
3	100	Full load	45.32	6.564	0.6065

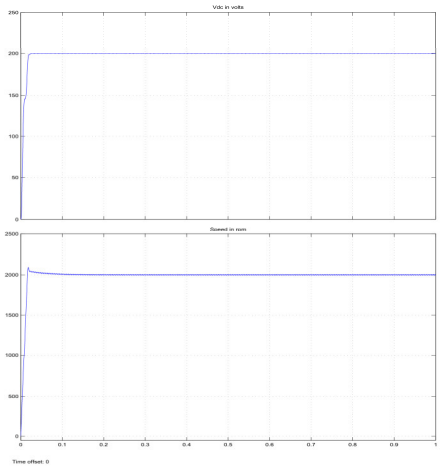

Figure 15 DC link voltage at 200 V and Speed of BLDC motor at rated load torque

Dynamic response

The dynamic response of the system by varying dc link voltage and load torque are shown in figures 18 and Figure 19 respectively. The dc link voltage is initially set to V_{dc} (= 200 V), around 0.5 second it is decreased to 50 % of V_{dc} (=100 V) and again around 0.8 second the voltage is raised to its V_{dc} (= 200V), the corresponding back emf, stator current and speed are given in Figure 18. Likewise initially the load torque is set to 50 % of the rated torque (0.75 Nm) and around 0.52 second it is increased to 100 % of the rated load torque (1.5 Nm), the corresponding back emf, stator current and speed are given in Figure 19. It is observed that the system settles quickly after the change in both the cases.

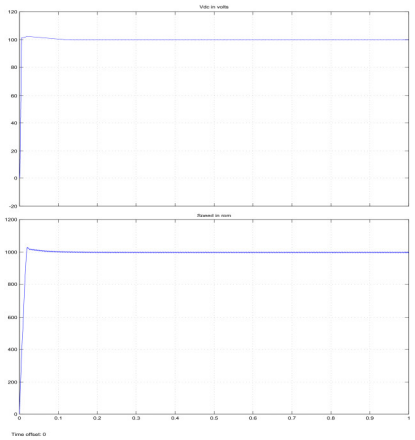

Figure 16 DC link voltage at 100 V and Speed of BLDC motor at rated load torque

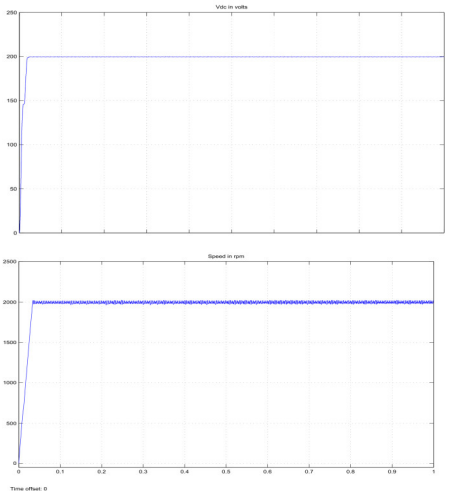

Figure 17 DC link voltage at 200 V and Speed of BLDC motor at 50 % rated load torque

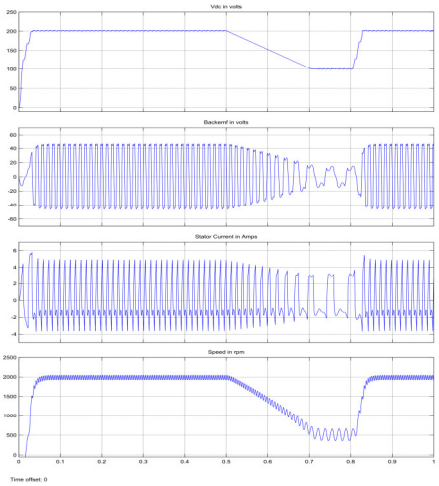

Figure 18 DC link variation of CSC converter fed BLDC motor

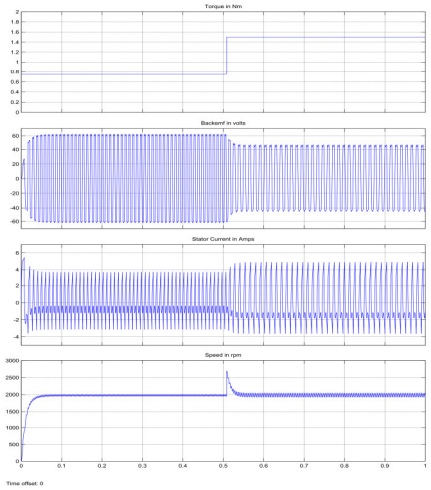

Figure 19 Load torque variation of CSC converter fed BLDC motor

VI. Landsman converter fed BLDC motor drive

Similar to CSC converter, Landsman converter also has variable dc link voltage. In landsman converter the input side inductor (L_{i1}, L_{i2}) current is discontinuous, while the voltage across the capacitor (C_1, C_2) and the current in the output side inductor (L_{o1}, L_{o2}) are continuous for any switching cycle.

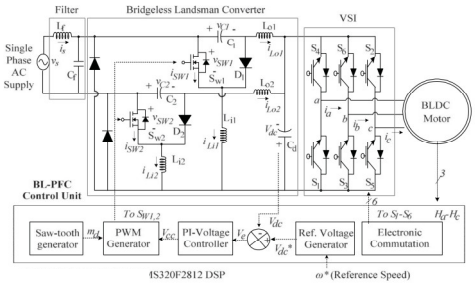

Figure 20 Landsman converter with BLDC motor drive

VII. Operation during complete switching period

The BL-Landsman converter is designed to oper ate in DICM such that current in inductor's L_{i1} and L_{i2} becomes discontinuous for a switching period by swit ching the corresponding switch for positive and negativ e half cycles of supply voltage. Figures 21 to 23 show s different modes of operation during a positive half c ycle of supply voltage.

Mode P1: The switch S_{w1} is turned ON and the energy out of the supply along with the energy stored in the intermittent capacitor C_1 is transported to input inductor L_{i1}. The output inductor L_{o1} starts settling and voltage of intermediary capacitor v_{C1} starts reducing while an input inductor current i_{Li1} and dc voltage V_{dc} start increasing. Calculated value of intermittent capacitance is adequate to retain suitable energy such that a continuous voltage is available throughout the operation

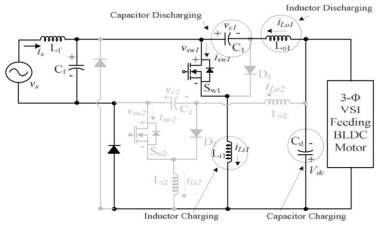

Figure 21 Mode P1

Mode P2: When the switch is turned OFF, the intermittent capacitor C_1 and dc bus side inductor L_{o1} start charging by the current from supply while input inductor L_{i1} jumps discharging; so, v_{C1} jumps increasing during this method.

Mode P3: in this mode the converter is working in the discontinuous conduction mode, as the input inductor L_{i1} is discharged and current iL_{i1} converts zero as shown in Figure 23. The output inductor current iL_{o1} is increasing while the intermediary capacitor voltage v_{C1} decreases in this mode.

For negative half cycle, the sequence of operation is similar to positive half cycle's mode 1,2 and 3 where the inductors L_{i2}, L_{o2} and capacitor C_2 operates instead of L_{i1}, L_{o1} and C_1 respectively.

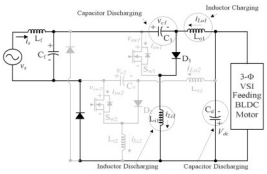

Figure 22 Mode P2

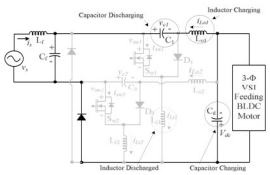

Figure 23 Mode P3

VIII. BL-Landsman converter design

As the Landsman converter is modified CSC converter and the modification is addition of an output inductor, converter given in CSC converter can be adopted for the converter's input inductor, intermittent capacitor and filter L-C values. Design of output inductor is given below,

Design of output Inductors

The value of the output inductors L_{o1} and L_{o2} for functioning in continuous conduction mode are determined considering the ripple current in the inductors [17] as given in (18).

$$L_{o1} = L_{o2} = \left(\frac{V_s^2}{P_i}\right)\frac{D}{\Delta i f_s} = \frac{1}{\Delta i f_s}\left(\frac{V_s^2}{P_i}\right)\left(\frac{V_{dc}}{V_{in}+V_{dc}}\right) \quad (18)$$

The allowed peak ripple current in the inductor occurs at rated V_{dc} for minimum V_s. Hence, the output inductor value is determined at maximum value of DC output with minimal input voltage.

$$L_{o1} = L_{o2} = \left(\frac{V_s^2}{P_i}\right)\frac{D}{\Delta i f_s} = \frac{1}{\Delta i f_s}\left(\frac{V_{s\,min}^2}{P_{i\,max}}\right)\left(\frac{V_{dc\,max}}{\sqrt{2}V_{s\,min}+V_{dc\,max}}\right)$$

$$L_{o1} = L_{o2} = \frac{1}{0.2 \times 20000} \frac{85^2}{500} \frac{200}{(\sqrt{2} \times 85)+200} = 2.25\ \text{mH}$$

Control of BL-Landsman converter fed BLDC motor drive

The control of the BL-CSC converter can be adopted for Landsman converter fed BLDC motor, since it is modified from it.

IX. Simulation of Landsman converter fed BLDC drive

The Simulink model of the Landsman converter fed brushless DC motor drive is given in Figure 24, the functional parameters such as back emf, stator current speed of the of the motor and DC link voltage of the converter are observed and presented in the figures 25 to 28.

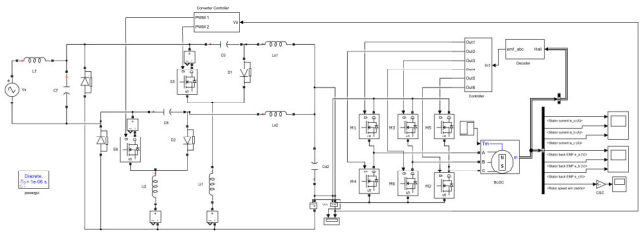

Figure 24 Simulink model of BL-Landsman fed BLDC drive

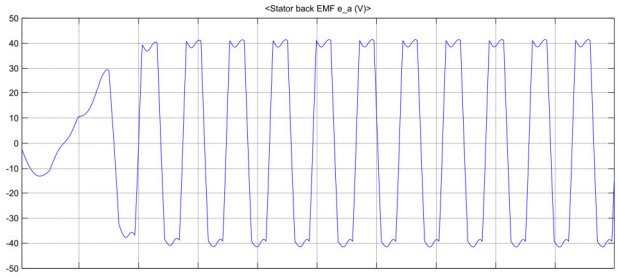

Figure 25 Stator back emf of Landsman converter fed BLDC motor

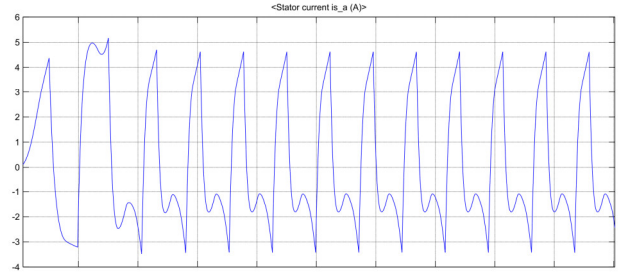

Figure 26 Stator current of Landsman converter fed BLDC motor

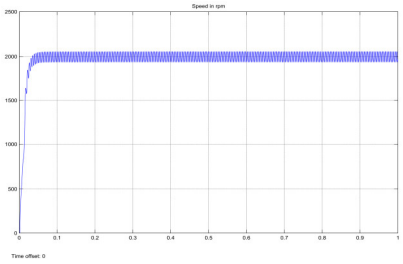

Figure 27 Speed Characteristics of Landsman converter fed BLDC drive

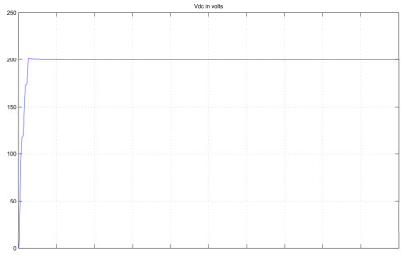

Figure 28 DC link voltage of CSC converter

Steady state response

The model is simulated with rated load torque with a dc link voltage of 200 V and 100 V, the corresponding speed and dc link voltage is given in Figure 29 and 30 respectively. Figure 31 gives speed characteristics of the model with 50 % of the rated load torque and a dc link voltage of 200 V. The time domain analysis in terms of integral square error, integral absolute error, integral time square error and integral time absolute error are obtained for the dc link voltage of the converter and speed of the motor in addition to ripple factor and are tabulated in Table 5 and Table 6 respectively.

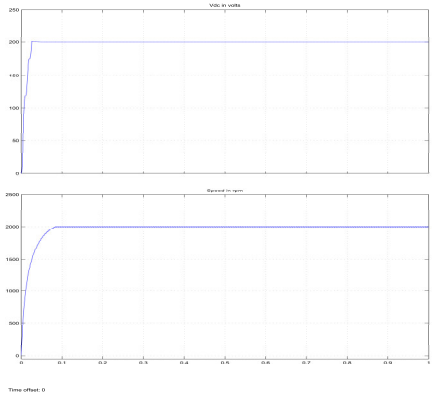

Figure 29 DC link voltage at 200 V and Speed of BLDC motor at rated load torque

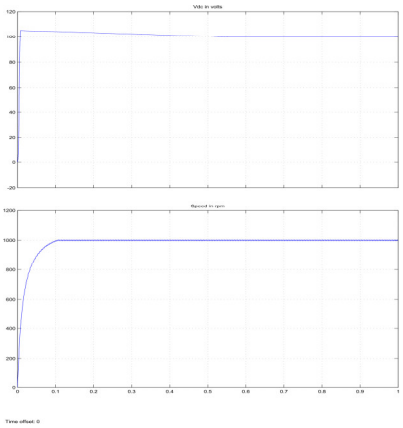

Figure 30 DC link voltage at 100 V and Speed of BLDC motor at rated load torque

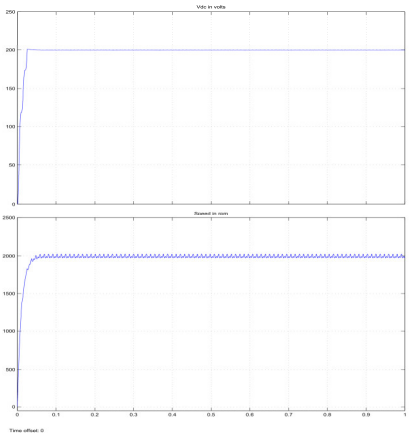

Figure 31 DC link voltage at 200 V and Speed of BLDC motor at 50 % rated load torque

Table 5 Summary of errors and ripple factor of V_{dc} of Landsman converter

S. No	DC link Voltage (V)	Load	IAE	ITAE	Ripple factor
1	200	Full load	2.22	0.1064	0.01189
2	200	½ load	2.251	0.1212	0.01355
3	100	Full load	1.809	0.2605	0.00252

Table 6 Summary of errors and ripple factor of BLDC motor's speed

S. No	DC link Voltage (V)	Load	IAE	ITAE	Ripple factor
1	200	Full load	39.8	2.648	0.2159
2	200	½ load	36.1	8.003	0.7805
3	100	Full load	21.2	1.421	0.1943

Dynamic response

The dynamic response of the system by varying dc link voltage and load torque are shown in figures 32 and Figure 33 respectively.

The dc link voltage is initially set to V_{dc} (= 200 V), around 0.4 second it is decreased to 50 % of V_{dc} (=100 V) and again around 0.8 second the voltage is raised to its V_{dc} (= 200V), the corresponding back emf, stator current and speed are given in Figure 32. Likewise initially the load torque is set to 50 % of the rated torque (0.75 Nm) and around 0.4 second it is increased to 100 % of the rated load torque (1.5 Nm), the corresponding back emf, stator current and speed are given in Figure 33. It is observed that the system settles quickly after the change in both the cases.

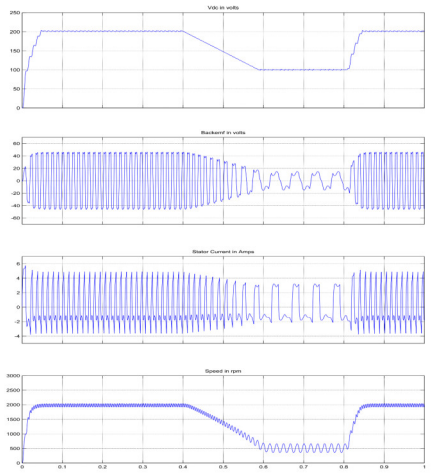

Figure 32 DC link variation of Landsman converter fed BLDC motor

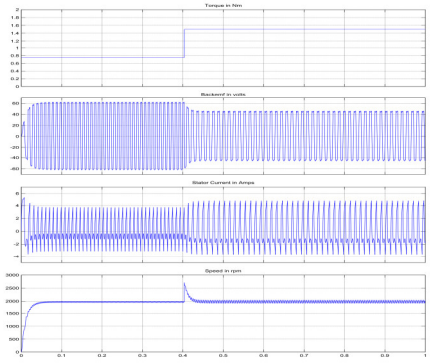

Figure 33 Load torque variation of Landsman converter fed BLDC motor.

Table 7 Comparison of errors and ripple factor of V_{dc} of Landsman converter

S. No	Converter	DC link Voltage (V)	Load	IAE	ITAE	Ripple factor
1	CSC	200	Full load	1.75	0.141	0.0268

S. No	Converter	DC link Voltage (V)	Load	IAE	ITAE	Ripple factor
2	Landsman	200	Full load	2.22	0.1064	0.01189
3	CSC	200	½ load	20.9	12.6	0.0817
4	Landsman	200	½ load	2.251	0.1212	0.01355
5	CSC	100	Full load	0.60	0.680	0.0212
6	Landsman	100	Full load	1.809	0.2605	0.00252

Table 8 Comparison of errors and ripple factor of BLDC motor's speed

S. No	Converter	DC link Voltage (V)	Load	IAE	ITAE	Ripple factor
1	CSC	200	Full load	39.8	2.648	0.2159
2	Landsman	200	Full load	20.75	1.598	0.1853
3	CSC	200	½ load	36.1	8.003	0.7805
4	Landsman	200	½ load	10.75	0.923	0.1792
5	CSC	100	Full load	21.2	1.421	0.1943
6	Landsman	100	Full load	45.32	6.564	0.6065

X. Conclusion

The analysis of canonical switching cell converter and landsman converter reveals that both the converters render appreciable performance in steady state and dynamic condition. The performance betterment is measure in terms of integral time absolute error and ripple factor of the dc link voltage and motor speed at converter output and drive accordingly. The analysis and comparison showcase that landsman converter fed BLDC drive have reduced error and ripple factor at converter output and in motor speed. This leads to conclude, Landsman converter fed BLDC drive offers better performance for different load conditions and speeds.

REFERENCES

[1] B. Singh and S. Singh, "Single-phase power factor controller topologies for permanent magnet brushless DC motor drives," IET Power Electronics, vol.3, no.2, pp.147-175, March 2010.

[2] Chang Liang Xia, Permanent Magnet Brushless DC Motor Drives and Controls, Wiley Press, Beijing, 2012.

[3] P. Pillay and R. Krishnan, "Modeling of permanent magnet motor drives," IEEE Trans. Ind. Elect., vol.35, no.4, pp.537-541, Nov 1988.

[4] M. A. Rahman and P. Zhou, "Analysis of brushless permanent magnet synchronous motors," IEEE Trans. Ind. Elect., vol.43, no.2, pp.256-267, Apr 1996.

[5] Xiaoyan Huang, A. Goodman, C. Gerada, Youtong Fang and Qinfen Lu,"A Single Sided Matrix Converter Drive for a Brushless DC Motor in Aerospace Applications," IEEE Trans. Ind. Elect., vol.59, no.9, pp.3542-3552, Sept. 2012.

[6] Santhosh, P., and Vijayakumar, P., Performance study of BLDC motor used in wireless medical application, Wireless Personal Communications, Vol. 94, No. 4, pp. 2451–2458.June 2017

[7] E. E. Landsman, "A unifying derivation of switching DC-DC converter topologies," in Proc. Power Electron. Spec. Conf. Record, San Diego, CA, USA, Jun. 18–22, 1979, pp. 239–243

[8] Santhosh P, Vijayakumar P and Sangaran D K,, "Applications of Brushless DC in Medical Applications", Innovative Technologies in Mechanical Engineering (ITME-2017), October 2017

[9] N. Mohan, T. M. Undeland and W. P. Robbins, Power Electronics: Converters, Applications and Design, John Wiley and Sons Inc, USA, 2003.

[10] Limits for Harmonic Current Emissions (Equipment input current ≤16 A per phase), International Standard IEC 61000-3-2, 2000

[11] . B. Singh, B. N. Singh, A. Chandra, K. Al-Haddad, A. Pandey and D.P. Kothari, "A review of single-phase improved power quality AC-DC converters," IEEE Trans. Ind. Elect., vol. 50, no. 5, pp. 962– 981, Oct. 2003.

[12] B. Singh, S. Singh, A. Chandra and K. Al-Haddad, "Comprehensive Study of Single-Phase AC-DC Power Factor Corrected Converters With High-Frequency Isolation," IEEE Trans. Ind. Inform., vol.7, no.4, pp.540-556, Nov. 2011.

[13] S.B.Ozturk, O. Yang and H. A. Toliyat, "Power factor correction of DTC controlled BLDC drive", 42nd IAS Annual Meeting and IEEE Industrial Applications Conference, pp.297-304, 23-27 Sept. 2007

[14] Chia-Hao Wu and Ying-Yu Tzou, "Digital control strategy for efficiency optimization of a BLDC motor driver with VOPFC," IEEE ECCE Conf., pp.2528-2534, 20-24 Sept. 2009.

[15] L. Cheng, "DSP-based variable speed motor drive with power factor correction and current harmonics compensation," 35th IECEC Conf., pp.1394-1399 vol.2, 2000

[16] B. K. Lee, B. Fahimi and M. Ehsani, "Overview of reduced parts converter topologies for AC motor drives," 32nd Annual IEEE Power Electron. Spec. Conf. (PESC) 2001, vol.4, pp.2019-2024, 2001.

[17] B. Singh and V. Bist, "A BL-CSC converter fed BLDC motor drive with power factor correction," IEEE Trans. Ind. Electron., vol. 62, no. 1, pp. 172–183, Jan. 2015

[18] Santhosh P., Suresh Kumaar G., Sangaran D. K. and Ranganathan T., "Review of High Voltage-Gain Bidirectional dc-dc Topologies", International Conference on Innovation in Signal Processing, Communication & Infromation Systems March 2018.

[19] P. K. Singh, B. Singh, V. Bist, A. Chandra, and K. Al-Haddad, "A single sensor based bridgeless landsman PFC converter fed BLDC motor drive," in Proc. 2015 IEEE Ind. Appl. Soc. Annu. Meeting, Addison, TX, USA, 2015, pp. 1–8.

[20] S. R. Paranjothi, C. S. Joice, and V. J. S. Kumar, "Digital control strategy for rour quadrant operation of three phase BLDC motor with load variations," IEEE Trans. Ind. Informat., vol. 9, no. 2, pp. 974–982,May 2013.
[21] L. Huber, Y. Jang and M.M Jovanovic, "Performance Evaluation of Bridgeless PFC Boost Rectifiers," IEEE Trans. Power Electron., vol.23, no.3, pp.1381-1390, May 2008.
[22] A. A. Fardoun, E. H. Ismail, M. A. Al-Saffar, and A. J. Sabzali, A.J., "New "real" bridgeless high efficiency AC-DC converter," 2012 Twenty-Seventh Annual IEEE Applied Power Electron. Conf. and Expos. (APEC), pp.317-323, 5-9 Feb. 2012.
[23] Wang Wei, Liu Hongpeng, Jiang Shigong and Xu Dianguo, "A novel bridgeless buck-boost PFC converter," IEEE Power Electron. Spec. Conf., (PESC) 2008. pp. 1304-1308, 15-19 June 2008.
[24] V. Bist and B. Singh, "An Adjustable Speed PFC Bridgeless Buck-Boost Converter Fed BLDC Motor Drive", IEEE Trans. Ind. Electron., vol.61, no.6, pp.2665-2677, June 2014.
[25] A. A. Fardoun, E. H. Ismail, A. J. Sabzali, M. A. Al-Saffar, "New Efficient Bridgeless Cuk Rectifiers for PFC Applications," IEEE Trans. Power Electron., vol.27, no.7, pp.3292-3301, July 2012.
[26] B. Singh and V. Bist, "An Improved Power Quality Bridgeless Cuk Converter Fed BLDC Motor Drive for Air Conditioning System", IET Power Elect., Volume 6, issue 5, pp. 902–913, 2013.
[27] M. Mahdavi and H. Farzaneh-Fard, "Bridgeless CUK power factor correction rectifier with reduced conduction losses," IET Power Electron., vol.5, no.9, pp.1733-1740, Nov. 2012.
[28] A. J. Sabzali, E. H. Ismail, M. A. Al-Saffar and A. A. Fardoun, "New Bridgeless DCM Sepic and Cuk PFC Rectifiers With Low Conduction and Switching Losses," IEEE Trans. Ind. Appl., vol.47, no.2, pp.873-881, March-April 2011.
[29] M. Mahdavi and H. Farzanehfard, "Bridgeless SEPIC PFC Rectifier with Reduced Components and Conduction Losses," IEEE Transactions on Industrial Electronics, vol.58, no.9, pp.4153-4160, Sept. 2011.
[30] V. Bist and B. Singh, "A Reduced Sensor PFC BL-Zeta Converter Based VSI Fed BLDC Motor Drive", Electric Power System Research, vol. 98, pp. 11–18, May 2013.
[31] O. Sago, K. Matsui, K, H. Mori, I. Yamamoto, M. Matsuo, I. Fujimatsu, Y. Watanabe and K. Ando, "An optimum single phase PFC circuit using CSC converter," 30th IEEE-IECON Conf. 2004, vol.3, pp. 2684-2689, 2-6 Nov. 2004.
[32] B. Williams, "Generation and Analysis of Canonical Switching Cell DCto-DC Converters," IEEE Trans. Ind. Electron., vol.61, no.1, pp.329-346, Jan. 2014.
[33] M. Matsuo, K. Matsui, I. Yamamoto and F. Ueda, "A comparison of various DC-DC converters and their application to power factor correction," 26th IEEE-IECON Conf., vol.2, pp.1007-1013, 2000.
[34] K. Matsui, I. Yamamoto, T. Kishi, M. Hasegawa, H. Mori and F. Ueda, "A comparison of various buck-boost converters and their application to PFC," 28th IEEE-IECON Conf., 2002, vol.1, pp. 30- 36, 5-8 Nov. 2002.
[35] D. S. L. Simonetti, J. Sebastian and J. Uceda, "The discontinuous conduction mode Sepic and Cuk power actor preregulators: analysis and design," IEEE Trans. Ind. Elect., vol. 44, no. 5, pp. 630-637, Oct. 1997.
[36] V. Vlatkovic, D. Borojevic and F. C. Lee, "Input Filter Design for Power Factor Correction Circuits," IEEE Trans. Power Elect., vol.11, no.1, pp.199-205, Jan 1996.
[37] P. Alaeinovin and J. Jatskevich, "Filtering of Hall-Sensor Signals for Improved Operation of Brushless DC Motors," IEEE Trans. Energy Convers. vol. 27, no. 2, June 2012.
[38] B. C. Kuo, Automatic Control Systems, PHI Learning, New Delhi, 2010.

Author Bibliography

P. Santhosh received his Bachelor of Engineering in Electrical and Electronics Engineering in 2008 from Anna University, Chennai and Master of Engineering in Power Electronics and Drives in 2011 from Karpagam University, Coimbatore and currently pursuing his PhD in Anna University, Chennai (part-time mode) and working as an Assistant Professor in the department of Electrical and Electronics Engineering of SVS College of Engineering, Coimbatore. He has a decade of teaching experience and nearly 20 publications to his credit in Journals and conferences. He is a recipient of best paper award for the paper 'Renewabl(E)nergy Locomotive' in 'The Ministry of New and Renewable Energy, Government of India' sponsored conference on 'Trends and Developments in Renewable Energy Sources', in 2009. His research interest includes Power electronic converters, Renewable energy, Special Electric Drives, virtual instrumentation, Automation and Soft computing. He is an active member of ISTE, ISRD IACSIT and IAENG.

Dr. P. Vijayakumar completed his Bachelor of Engineering in Electrical and Electronics Engineering in 1992 and Master of Engineering in Applied Electronics in 2002 from PSG College of Technology, Coimbatore (Bharathiar University, Coimbatore) and PhD in 2007 from Anna University, Chennai. He is currently working as Professor in Electrical and Electronics Engineering and Principal of Karpagam College of Engineering. Coimbatore, India. He has nearly 100 publication to his credit in National and International Conference/Journals. He has guided 8 research scholars and currently 8 more are pursuing research under his eminent guidance. He has more than two decades of experience in industry and Teaching. His research interests include Low-power VLSI design, Virtual instrumentation, Power Electronic Drives, and Soft computing. He is an active member of IEEE, ISTE, VSI and SSI.